



A study of global dynamics and sensitivity analysis of a discrete-time model of the COVID-19 epidemic

M. E.-B. Keddar and O. Belhamiti*, 

Abstract

This study presents a novel approach to understanding the global dynamics of COVID-19 transmission with vaccination based on a discrete-time model. We establish biologically meaningful constraints on the model parameters and prove the existence of a disease-free equilibrium and an endemic equilibrium under these constraints, along with their theoretical stabilities. Furthermore, we identify the most sensitive operational parameters that have a substantial impact on the transmission of the epidemic. Through numerical simulations, we demonstrate the local stability of the two equilibria, depending on the parameter values. Our findings reveal that the discrete-time model is not only dynamically robust but also more

*Corresponding author

Received 14 June 2023; revised 3 November 2023; accepted 6 November 2023

Meriem El-Batoul Keddar

Department of Mathematics and Computer Science, Abdelhamid Ibn Badis Mostaganem University, Algeria. e-mail: batoulkeddar@gmail.com

Omar Belhamiti

Department of Mathematics and Computer Science, Abdelhamid Ibn Badis Mostaganem University, Algeria. e-mail: omar.belhamiti@univ-mosta.dz

How to cite this article

Keddar, M. E.-B. and Belhamiti, O., A study of global dynamics and sensitivity analysis of a discrete-time model of the COVID-19 epidemic. *Iran. J. Numer. Anal. Optim.*, 2024; 14(1): 136-171. <https://doi.org/10.22067/ijnao.2023.82954.1281>

realistic than its continuous counterpart under biologically meaningful constraints. These results provide a foundation for future research in this area and contribute to our understanding of the global dynamics of COVID-19 transmission.

AMS subject classifications (2020): Primary 39A12; Secondary 92C60, 92D30.

Keywords: Discrete-time epidemic model; Euler Scheme, Local stability; Vaccination reproduction number.

1 Introduction and Motivation

Coronaviruses are a family of viruses that cause respiratory and intestinal infections in humans and animals [6]. They were not dangerous to humans until the appearance of severe acute respiratory syndrome coronavirus (SARS-CoV) in 2002 in China [16]. This virus had infected 8,096 people in 25 countries, causing 774 deaths [19]. A decade later, the outbreak of another highly pathogenic coronavirus, Middle East respiratory syndrome coronavirus (MERS-CoV), occurred in Jeddah, Saudi Arabia [32]. The virus spread, infecting more than 2,400 people in 27 countries and causing over 850 deaths [13]. In December 2019, a third of these dangerous coronaviruses appeared in the city of Wuhan, China. Forty-four cases were reported in this country on January 3, 2020 [24]. The virus migrated to neighboring regions and countries. In less than a month, 106 confirmed cases were detected in 19 different countries, and the number of infected individuals reached 9,826, with 213 deaths. The World Health Organization (WHO) declared the outbreak to be a public health emergency of international concern [24]. The Severe Acute Respiratory Syndrome Coronavirus 2 (SARS-CoV-2) is the virus that caused this disease, which has spread throughout the world. It was named COVID-19 by the WHO [23], which declared that this malady can be characterized as a pandemic [25]. On April 4, 2020, the number of infected people exceeded 1 million, with 56,986 deaths worldwide [26]. Many countries have gone into total confinement and closed their borders to reduce the spread of the virus. The number of infected people increases more and more rapidly over time.

In December of the following year, more than 75 million confirmed cases and 1.6 million deaths have been reported globally [27]. As of November 2022, COVID-19 still exists, and its spread worldwide has resulted in 629 million confirmed cases and 6.5 million deaths [28]. The number is increasing even now.

This pandemic has left the world feeling helpless due to its rapid spread and the lack of specific medicines or treatments available to combat it. As a result, many countries have implemented non-pharmaceutical measures, such as confinement, mask-wearing, social distancing, isolation, and treatment of infected persons, in an attempt to contain the virus. However, the effectiveness of these measures has proven to be limited. This has prompted epidemiologists to develop vaccines as a solution. Many of the developed vaccines are safe and effective in providing protection against severe forms of COVID-19, offering a glimmer of hope for an end to this pandemic that has impacted humanity for over two years. The COVID-19 pandemic has affected all sectors of health and security, including the involvement of mathematicians to control and stop its spread. Numerous mathematical models have been proposed, allowing for the control of the pandemic, prediction of its evolution, and estimation of key transmission parameters, such as the basic reproduction number R_0 , as well as analyzing the impact of vaccines on disease dynamics. Most of these mathematical models are nonlinear continuous-time systems of the SEIR type, which study the dynamic transmission of COVID-19, such as those presented in [21, 12, 15]. Some models also include vaccination, as seen in [1, 31, 30]. However, only a few models are discretized-time models.

It should be noted that discrete-time models present a great advantage compared to continuous-time models, especially for COVID-19, as the individual goes through several phases (Susceptible-Exposed-Infected ...) and the phases of the disease represent the step of discretization, which can vary between five days to a week, depending on the individual. Despite these considerations, only a few articles have been published in discrete time that take into account the disease phases. In [8], the authors proposed a SEIR model with several characteristics. Firstly, the exposed subpopulation is infectious. They also incorporated a feedback vaccination control law on the susceptible. Furthermore, the model is subject to delayed partial re-susceptibility,

meaning that a partial immunity loss in the recovered individuals occurs after some time. By the same authors in [9], a new discrete SEIR model has been developed. This model considers the injection of two doses with different delays and a possible average different effectiveness. It also considers that the exposed have a transmission rate exposed-susceptible, which may be eventually distinct from the infectious-susceptible transmission rate. In [2], the authors proposed a new SIR model with vaccination. Their model has two equilibrium points, namely, a disease-free equilibrium (DFE) and an endemic equilibrium. By considering both the forward difference system and the backward difference system, some stability analyses of the DFE point are performed.

This paper describes a new discrete SEIR model for COVID-19 transmission dynamics that include vaccination. The model assumes that only symptomatic and asymptomatic infected individuals can transmit the disease and that hospitalized patients are isolated. It also considers the possibility of reinfection with the virus, as the vaccine may not be fully protective. [4]. Some exposed and asymptomatic infected can be vaccinated; this is due to the inefficiency of the tests [29]. The vaccination reproduction number R_v and the equilibrium points are calculated, and their sensibility and stability analysis are studied. Numerical simulations are performed considering various scenarios. We present detailed results in the form of graphs and tables, including new numerical results obtained for model validation.

The paper is organized as follows. Section 2 introduces the mathematical model and provides a preliminary overview. In section 3, the mathematical analysis is carried out to investigate the stability of the proposed model. This section focuses on the study of equilibrium points and their stability properties. Section 4 presents a sensitivity analysis of the model to investigate how changes in the model parameters affect the system behavior. Finally, section 5 presents the results and discussions of the model simulations, which provide insights into the system's behavior and its implications.

2 Mathematical model

In this section, we use the explicit Euler scheme to obtain a discrete-time model for the transmission of COVID-19. Based on the epidemiological status and the timeline of COVID-19 infection in [18], the population is divided as follows:

- **S** is the susceptible class,
- **E** is the exposed class, for example, the people in the incubation period,
- **V** is the vaccinated class,
- **I^a** is the asymptomatic infected class,
- **I^s** is a class of individuals diagnosed with moderate COVID-19 symptoms, which is further divided into two subclasses I^{s1} refers to individuals experiencing symptoms in their first phase (i.e., within a week of symptom onset), as described in [11, 17] while I^{s2} refers to individuals experiencing symptoms in their second phase (i.e., roughly one week after the end of the first phase of symptoms), also documented in references [11, 17]. That is,

$$\mathbf{I}^s = \mathbf{I}^{s1} + \mathbf{I}^{s2}.$$

- **I^h** refers to the class of infected individuals who require hospitalization, including those who need intensive care. This class is further subdivided into three subclasses based on the interval since symptom onset: \mathbf{I}^{h1} represents individuals who are hospitalized within a week of symptom onset, as detailed in references [11, 17], while \mathbf{I}^{h2} denotes those who are hospitalized around one week after the end of the first phase of symptoms. Lastly, \mathbf{I}^{h3} pertains to individuals who are hospitalized approximately one week after the end of the second phase of symptoms, also documented in references [11, 17]. That is,

$$\mathbf{I}^h = \mathbf{I}^{h1} + \mathbf{I}^{h2} + \mathbf{I}^{h3}.$$

- **R** represents the class of individuals who have recovered from COVID-19.
- **D** represents the class of individuals who have died from COVID-19.

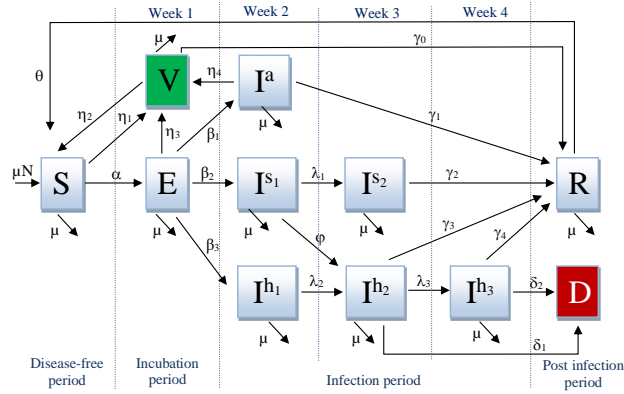


Figure 1: Timeline of infection and states transition scheme description.

By applying the explicit Euler scheme, we can obtain a discretized SEIR epidemic model that incorporates vaccination (see Figure 1). Considering the week-long interval required for individuals to transition between classes, the resulting model is as follows:

$$\left\{ \begin{array}{l}
 \mathbf{S}(t+1) = \mathbf{S}(t) + \mu N - \eta_1 \mathbf{S}(t) + \eta_2 \mathbf{V}(t) + \theta \mathbf{R}(t) - \mu \mathbf{S}(t) \\
 \quad - \alpha \mathbf{S}(t) \frac{(\mathbf{I}^a(t) + \mathbf{I}^{s1}(t) + \mathbf{I}^{s2}(t))}{N}, \\
 \mathbf{E}(t+1) = \mathbf{E}(t) + \alpha \mathbf{S}(t) \frac{(\mathbf{I}^a(t) + \mathbf{I}^{s1}(t) + \mathbf{I}^{s2}(t))}{N} \\
 \quad - (\beta_1 + \beta_2 + \beta_3 + \eta_3 + \mu) \mathbf{E}(t), \\
 \mathbf{V}(t+1) = \mathbf{V}(t) + \eta_1 \mathbf{S}(t) + \eta_3 \mathbf{E}(t) + \eta_4 \mathbf{I}^a(t) - (\eta_2 + \gamma_0 + \mu) \mathbf{V}(t), \\
 \mathbf{I}^a(t+1) = \mathbf{I}^a(t) + \beta_1 \mathbf{E}(t) - (\eta_4 + \gamma_1 + \mu) \mathbf{I}^a(t), \\
 \mathbf{I}^{s1}(t+1) = \mathbf{I}^{s1}(t) + \beta_2 \mathbf{E}(t) - (\lambda_1 + \varphi + \mu) \mathbf{I}^{s1}(t), \\
 \mathbf{I}^{s2}(t+1) = \mathbf{I}^{s2}(t) + \lambda_1 \mathbf{I}^{s1}(t) - (\gamma_2 + \mu) \mathbf{I}^{s2}(t), \\
 \mathbf{I}^{h1}(t+1) = \mathbf{I}^{h1}(t) + \beta_3 \mathbf{E}(t) - (\lambda_2 + \mu) \mathbf{I}^{h1}(t), \\
 \mathbf{I}^{h2}(t+1) = \mathbf{I}^{h2}(t) + \lambda_2 \mathbf{I}^{h1}(t) + \varphi \mathbf{I}^{s1}(t) - (\lambda_3 + \gamma_3 + \delta_1 + \mu) \mathbf{I}^{h2}(t), \\
 \mathbf{I}^{h3}(t+1) = \mathbf{I}^{h3}(t) + \lambda_3 \mathbf{I}^{h2}(t) - (\gamma_4 + \delta_2 + \mu) \mathbf{I}^{h3}(t), \\
 \mathbf{R}(t+1) = \mathbf{R}(t) + \gamma_0 \mathbf{V}(t) + \gamma_1 \mathbf{I}^a(t) + \gamma_2 \mathbf{I}^{s2}(t) + \gamma_3 \mathbf{I}^{h2}(t) \\
 \quad + \gamma_4 \mathbf{I}^{h3}(t) - (\theta + \mu) \mathbf{R}(t), \\
 \mathbf{D}(t+1) = \mathbf{D}(t) + \delta_1 \mathbf{I}^{h2}(t) + \delta_2 \mathbf{I}^{h3}(t),
 \end{array} \right. \quad (1)$$

We assume that the total population N remains constant,

$$N(t+1) = N(t).$$

Taking into account the previous assumption, we can normalize the variables in the model (1),

$$\begin{aligned} S(t) &= \frac{\mathbf{S}(t)}{N}, & E(t) &= \frac{\mathbf{E}(t)}{N}, & V(t) &= \frac{\mathbf{V}(t)}{N}, & I^a(t) &= \frac{\mathbf{I}^a(t)}{N}, \\ I^{s_1}(t) &= \frac{\mathbf{I}^{s_1}(t)}{N}, & I^{s_2}(t) &= \frac{\mathbf{I}^{s_2}(t)}{N}, & I^{h_1}(t) &= \frac{\mathbf{I}^{h_1}(t)}{N}, & I^{h_2}(t) &= \frac{\mathbf{I}^{h_2}(t)}{N}, \\ I^{h_3}(t) &= \frac{\mathbf{I}^{h_3}(t)}{N}, & R(t) &= \frac{\mathbf{R}(t)}{N}, & D(t) &= \frac{\mathbf{D}(t)}{N}. \end{aligned}$$

Because

$$\begin{aligned} S(t) + E(t) + V(t) + I^a(t) + I^{s_1}(t) + I^{s_2}(t) \\ + I^{h_1}(t) + I^{h_2}(t) + I^{h_3}(t) + R(t) + D(t) = 1, \end{aligned}$$

then

$$\begin{aligned} D(t) = 1 - (S(t) + E(t) + V(t) + I^a(t) + I^{s_1}(t) \\ + I^{s_2}(t) + I^{h_1}(t) + I^{h_2}(t) + I^{h_3}(t) + R(t)). \end{aligned}$$

Then, we have the following normalized reduced system:

$$\left\{ \begin{aligned} S(t+1) &= S(t) + \mu - \eta_1 S(t) + \eta_2 V(t) + \theta R(t) - \mu S(t) \\ &\quad - \alpha S(t) (I^a(t) + I^{s_1}(t) + I^{s_2}(t)), \\ E(t+1) &= E(t) + \alpha S(t) (I^a(t) + I^{s_1}(t) + I^{s_2}(t)) \\ &\quad - (\beta_1 + \beta_2 + \beta_3 + \eta_3 + \mu) E(t), \\ V(t+1) &= V(t) + \eta_1 S(t) + \eta_3 E(t) + \eta_4 I^a(t) - (\eta_2 + \gamma_0 + \mu) V(t), \\ I^a(t+1) &= I^a(t) + \beta_1 E(t) - (\eta_4 + \gamma_1 + \mu) I^a(t), \\ I^{s_1}(t+1) &= I^{s_1}(t) + \beta_2 E(t) - (\lambda_1 + \varphi + \mu) I^{s_1}(t), \\ I^{s_2}(t+1) &= I^{s_2}(t) + \lambda_1 I^{s_1}(t) - (\gamma_2 + \mu) I^{s_2}(t), \\ I^{h_1}(t+1) &= I^{h_1}(t) + \beta_3 E(t) - (\lambda_2 + \mu) I^{h_1}(t), \\ I^{h_2}(t+1) &= I^{h_2}(t) + \lambda_2 I^{h_1}(t) + \varphi I^{s_1}(t) - (\lambda_3 + \gamma_3 + \delta_1 + \mu) I^{h_2}(t), \\ I^{h_3}(t+1) &= I^{h_3}(t) + \lambda_3 I^{h_2}(t) - (\gamma_4 + \delta_2 + \mu) I^{h_3}(t), \\ R(t+1) &= R(t) + \gamma_0 V(t) + \gamma_1 I^a(t) + \gamma_2 I^{s_2}(t) + \gamma_3 I^{h_2}(t) \\ &\quad + \gamma_4 I^{h_3}(t) - (\theta + \mu) R(t), \end{aligned} \right. \quad (2)$$

where

μ represents the natural mortality,

α represents the transmission rate of COVID-19,

$(\eta_i)_{i=\overline{1,3,4}}$ represent the vaccination rates for each class,

$(\beta_i)_{i=\overline{1,3}}$ represent the rates at which exposed individuals become infected,

$(\gamma_i)_{i=\overline{0,4}}$ represent the recovery rates from each class,

$(\lambda_i)_{i=\overline{1,3}}$ represent the rates of transition from one class to another,

$(\delta_i)_{i=1,2}$ signify COVID-19 mortality rates per hospitalized group,

θ and η_2 denote COVID-19 reinfection rates, and

φ represents the hospitalization rate in the symptomatic phase I^{s_1} .

It is essential to assume that all model parameters are positive. Furthermore, some conditions on these parameters are necessary to ensure that the model has biological significance. In the following subsection, we present and illustrate these conditions.

2.1 Positive invariant set

The domain

$$\Omega = \{(S, E, V, I^a, I^{s_1}, I^{s_2}, I^{h_1}, I^{h_2}, I^{h_3}, R) \in \mathbb{R}_+^{10} : \\ 0 \leq S + E + V + I^a + I^{s_1} + I^{s_2} + I^{h_1} + I^{h_2} + I^{h_3} + R \leq 1\}$$

is a positive invariant set for system (2).

To render the model biologically meaningful, it is imperative to exhibit the belonging of solutions from the system (2) into Ω . This, in turn, hinges on ensuring that the combined outflow rates for each state do not surpass 1, as follows:

$$\left\{ \begin{array}{l} \eta_1 + \alpha + \mu \leq 1, \\ \beta_1 + \beta_2 + \beta_3 + \eta_3 + \mu \leq 1, \\ \eta_2 + \gamma_0 + \mu \leq 1, \\ \eta_4 + \gamma_1 + \mu \leq 1, \\ \lambda_1 + \varphi + \mu \leq 1, \end{array} \right. \quad \text{and} \quad \left\{ \begin{array}{l} \gamma_2 + \mu \leq 1, \\ \lambda_2 + \mu \leq 1, \\ \lambda_3 + \gamma_3 + \delta_1 + \mu \leq 1, \\ \gamma_4 + \delta_2 + \mu \leq 1, \\ \theta + \mu \leq 1. \end{array} \right.$$

Let $(S_n, E_n, V_n, I_n^a, I_n^{s_1}, I_n^{s_2}, I_n^{h_1}, I_n^{h_2}, I_n^{h_3}, R_n) \in \Omega$. Then, we have

$$\left\{ \begin{array}{l} S_{n+1} = S_n + \mu - \eta_1 S_n + \eta_2 V_n + \theta R_n - \alpha S_n (I_n^a + I_n^{s1} + I_n^{s2}) - \mu S_n \\ \qquad \geq \mu + (1 - (\eta_1 + \alpha + \mu)) S_n \geq 0, \\ E_{n+1} = E_n + \alpha S_n (I_n^a + I_n^{s1} + I_n^{s2}) - (\beta_1 + \beta_2 + \beta_3 + \eta_3 + \mu) E_n \\ \qquad \geq (1 - (\beta_1 + \beta_2 + \beta_3 + \eta_3 + \mu)) E_n \geq 0, \\ V_{n+1} = V_n + \eta_1 S_n + \eta_3 E_n + \eta_4 I_n^a - (\eta_2 + \gamma_0 + \mu) V_n \\ \qquad \geq (1 - (\eta_2 + \gamma_0 + \mu)) V_n \geq 0, \\ I_{n+1}^a = I_n^a + \beta_1 E_n - (\eta_4 + \gamma_1 + \mu) I_n^a \\ \qquad \geq (1 - (\eta_4 + \gamma_1 + \mu)) I_n^a \geq 0, \\ I_{n+1}^{s1} = I_n^{s1} + \beta_2 E_n - (\lambda_1 + \varphi + \mu) I_n^{s1} \\ \qquad \geq (1 - (\lambda_1 + \varphi + \mu)) I_n^{s1} \geq 0, \\ I_{n+1}^{s2} = I_n^{s2} + \lambda_1 I_n^{s1} - (\gamma_2 + \mu) I_n^{s2} \\ \qquad \geq (1 - (\gamma_2 + \mu)) I_n^{s2} \geq 0, \\ I_{n+1}^{h1} = I_n^{h1} + \beta_3 E_n - (\lambda_2 + \mu) I_n^{h1} \\ \qquad \geq (1 - (\lambda_2 + \mu)) I_n^{h1} \geq 0, \\ I_{n+1}^{h2} = I_n^{h2} + \lambda_2 I_n^{h1} + \varphi I_n^{s1} - (\lambda_3 + \gamma_3 + \delta_1 + \mu) I_n^{h2} \\ \qquad \geq (1 - (\lambda_3 + \gamma_3 + \delta_1 + \mu)) I_n^{h2} \geq 0, \\ I_{n+1}^{h3} = I_n^{h3} + \lambda_3 I_n^{h2} - (\gamma_4 + \delta_2 + \mu) I_n^{h3} \\ \qquad \geq (1 - (\gamma_4 + \delta_2 + \mu)) I_n^{h3} \geq 0, \\ R_{n+1} = R_n + \gamma_0 V_n + \gamma_1 I_n^a + \gamma_2 I_n^{s2} + \gamma_3 I_n^{h2} + \gamma_4 I_n^{h3} - (\theta + \mu) R_n \\ \qquad \geq (1 - (\theta + \mu)) R_n \geq 0. \end{array} \right.$$

Thus,

$$S_{n+1} + E_{n+1} + V_{n+1} + I_{n+1}^a + I_{n+1}^{s1} + I_{n+1}^{s2} + I_{n+1}^{h1} + I_{n+1}^{h2} + I_{n+1}^{h3} + R_{n+1} \geq 0.$$

On the other hand, the sum of the system equations (2) gives

$$\begin{aligned} S_{n+1} + E_{n+1} + V_{n+1} + I_{n+1}^a + I_{n+1}^{s1} + I_{n+1}^{s2} + I_{n+1}^{h1} + I_{n+1}^{h2} + I_{n+1}^{h3} + R_{n+1} \\ = \mu + (1 - \mu) (S_n + E_n + V_n + I_n^a + I_n^{s1} + I_n^{s2} + I_n^{h1} + I_n^{h2} + I_n^{h3} + R_n) - (\delta_1 I_n^{h2} + \delta_2 I_n^{h3}) \\ \leq \mu + (1 - \mu) (S_n + E_n + V_n + I_n^a + I_n^{s1} + I_n^{s2} + I_n^{h1} + I_n^{h2} + I_n^{h3} + R_n) \\ \leq \mu + (1 - \mu) \leq 1. \end{aligned}$$

Finally, we can say that

$$\left(S_{n+1}, E_{n+1}, V_{n+1}, I_{n+1}^a, I_{n+1}^{s1}, I_{n+1}^{s2}, I_{n+1}^{h1}, I_{n+1}^{h2}, I_{n+1}^{h3}, R_{n+1} \right) \in \Omega.$$

2.2 Vaccination reproduction number R_v

The basic reproduction number, R_v , is a fundamental epidemiological parameter that quantifies the contagiousness of an infectious disease. It represents the average number of secondary infections generated by one infected person in a susceptible population. If R_v is greater than 1, then the disease can sustain transmission; if it is less than 1, then it is likely to die out.

In this subsection, we describe the method used to estimate the vaccination reproduction number R_v (also called a control reproduction number) for our SEIR-V model. This method, proposed by Diekmann, Heesterbeek, and Metz [10], and further elaborated by Van Den Driessche and Watmough [22], involves using the next-generation matrix to determine R_v for an ordinary differential equation compartmental model.

Starting from the system (2), we can obtain the nontrivial DFE point as follows (is calculated in the next section):

$$E_0 = \left(S^*, 0, \frac{\eta_1 S^*}{(\eta_2 + \gamma_0 + \mu)}, 0, 0, 0, 0, 0, 0, \frac{\gamma_0 \eta_1 S^*}{(\theta + \mu)(\eta_2 + \gamma_0 + \mu)} \right)$$

with

$$S^* = \frac{(\theta + \mu)(\eta_2 + \gamma_0 + \mu)}{(\theta + \mu)(\eta_2 + \gamma_0 + \mu) + \eta_1(\theta + \mu) + \eta_1 \gamma_0}.$$

Let $X = (E, V, I^a, I^{s_1}, I^{s_2}, I^{h_1}, I^{h_2}, I^{h_3})^T$. Then the model can be written as

$$\begin{aligned} X(t+1) - X(t) &= \mathcal{F}(X(t)) - \mathcal{V}(X(t)) \\ &= \begin{pmatrix} \alpha S(t)(I^a(t) + I^{s_1}(t) + I^{s_2}(t)) - (\beta_1 + \beta_2 + \beta_3 + \eta_3 + \mu)E(t) \\ \eta_1 S(t) + \eta_3 E(t) + \eta_4 I^a(t) - (\eta_2 + \gamma_0 + \mu)V(t) \\ \beta_1 E(t) - (\eta_4 + \gamma_1 + \mu)I^a(t) \\ \beta_2 E(t) - (\lambda_1 + \varphi + \mu)I^{s_1}(t) \\ \lambda_1 I^{s_1}(t) - (\gamma_2 + \mu)I^{s_2}(t) \\ \beta_3 E(t) - (\lambda_2 + \mu)I^{h_1}(t) \\ \lambda_2 I^{h_1}(t) + \varphi I^{s_1}(t) - (\lambda_3 + \gamma_3 + \delta_1 + \mu)I^{h_2}(t) \\ \lambda_3 I^{h_2}(t) - (\gamma_4 + \delta_2 + \mu)I^{h_3}(t) \end{pmatrix}. \end{aligned}$$

We represent $\mathcal{F}(X)$ as the rate of appearance of new infections in each compartment, while $\mathcal{V}(X)$ signifies the disparity between the rate of individuals leaving each compartment and the rate of individuals entering the same compartment through all other means. It is assumed that each function is continuously differentiable at least twice in each variable. So, we have

$$\mathcal{F}(X) = \begin{pmatrix} \alpha S(I^a + I^{s_1} + I^{s_2}) \\ 0 \\ 0 \\ 0 \\ 0 \\ 0 \\ 0 \\ 0 \end{pmatrix}$$

and

$$\mathcal{V}(X) = \begin{pmatrix} (\beta_1 + \beta_2 + \beta_3 + \eta_3 + \mu) E \\ (\eta_2 + \gamma_0 + \mu) V - \eta_1 S - \eta_3 E - \eta_4 I^a \\ (\eta_4 + \gamma_1 + \mu) I^a - \beta_1 E \\ (\lambda_1 + \varphi + \mu) I^{s_1} - \beta_2 E \\ (\gamma_2 + \mu) I^{s_2} - \lambda_1 I^{s_1} \\ (\lambda_2 + \mu) I^{h_1} - \beta_3 E \\ (\lambda_3 + \gamma_3 + \delta_1 + \mu) I^{h_2} - \lambda_2 I^{h_1} - \varphi I^{s_1} \\ (\gamma_4 + \delta_2 + \mu) I^{h_3} - \lambda_3 I^{h_2} \end{pmatrix}.$$

The vaccination reproduction number, R_v , is calculated by next generation technique. The \tilde{F} and \tilde{V} matrices at DFE is given as follows:

$$F = \frac{\partial \mathcal{F}(X)}{\partial X} \Big|_{E_0} = \alpha S^* \begin{pmatrix} 0 & 0 & 1 & 1 & 1 & 0 & 0 & 0 \\ 0 & 0 & 0 & 0 & 0 & 0 & 0 & 0 \\ 0 & 0 & 0 & 0 & 0 & 0 & 0 & 0 \\ 0 & 0 & 0 & 0 & 0 & 0 & 0 & 0 \\ 0 & 0 & 0 & 0 & 0 & 0 & 0 & 0 \\ 0 & 0 & 0 & 0 & 0 & 0 & 0 & 0 \\ 0 & 0 & 0 & 0 & 0 & 0 & 0 & 0 \\ 0 & 0 & 0 & 0 & 0 & 0 & 0 & 0 \end{pmatrix}$$

and

$$V = \frac{\partial \mathcal{V}(X)}{\partial X} \Big|_{X=E_0},$$

where

$$\begin{cases} V_{1,1} = (\beta_1 + \beta_2 + \beta_3 + \eta_3 + \mu), \\ V_{2,1} = -\eta_3, \\ V_{3,1} = -\beta_1, \\ V_{4,1} = -\beta_2, \\ V_{6,1} = -\beta_3, \\ V_{2,2} = (\eta_2 + \gamma_0 + \mu), \\ V_{2,3} = -\eta_4, \\ V_{3,3} = (\eta_4 + \gamma_1 + \mu), \\ V_{4,4} = (\lambda_1 + \varphi + \mu), \end{cases} \begin{cases} V_{5,4} = -\lambda_1, \\ V_{5,5} = (\gamma_2 + \mu), \\ V_{6,6} = (\lambda_2 + \mu), \\ V_{7,4} = -\varphi, \\ V_{7,6} = -\lambda_2, \\ V_{7,7} = (\lambda_3 + \gamma_3 + \delta_1 + \mu), \\ V_{8,7} = -\lambda_3, \\ V_{8,8} = (\gamma_4 + \delta_2 + \mu), \\ 0 \quad \text{otherwise.} \end{cases}$$

Therefore, the next generation matrix is

$$\begin{cases} (FV^{-1})_{1,1} = \frac{\alpha}{(\beta_1 + \beta_2 + \beta_3 + \eta_3 + \mu)} \left(\frac{\beta_1}{(\eta_4 + \gamma_1 + \mu)} + \frac{\beta_2(\gamma_2 + \mu) + \lambda_1\beta_2}{(\lambda_1 + \varphi + \mu)(\gamma_2 + \mu)} \right) S^*, \\ (FV^{-1})_{1,3} = \frac{\alpha}{(\eta_4 + \gamma_1 + \mu)} S^*, \\ (FV^{-1})_{1,4} = \left(1 + \frac{\lambda_1}{(\gamma_2 + \mu)} \right) \frac{\alpha S^*}{(\lambda_1 + \varphi + \mu)}, \\ (FV^{-1})_{1,5} = \frac{\alpha S^*}{(\gamma_2 + \mu)}, \\ 0 \quad \text{otherwise.} \end{cases}$$

According to Van Den Driessche and Watmough [22], the vaccination reproduction number, R_v , is the spectral radius of the next generation matrix, which is given by

$$R_v = \alpha S^* \frac{\beta_2(\eta_4 + \gamma_1 + \mu)(\gamma_2 + \mu) + \beta_1(\lambda_1 + \varphi + \mu)(\gamma_2 + \mu) + \lambda_1\beta_2(\eta_4 + \gamma_1 + \mu)}{(\beta_1 + \beta_2 + \beta_3 + \eta_3 + \mu)(\eta_4 + \gamma_1 + \mu)(\lambda_1 + \varphi + \mu)(\gamma_2 + \mu)}, \quad (3)$$

where

$$S^* = \frac{(\theta + \mu)(\eta_2 + \gamma_0 + \mu)}{(\theta + \mu)(\eta_2 + \gamma_0 + \mu + \eta_1) + \eta_1\gamma_0},$$

2.3 Equilibrium points

The equilibrium points for the model (2) can be obtained by solving the following equations:

$$S(t+1) - S(t) = E(t+1) - E(t) = V(t+1) - V(t) = 0$$

$$\begin{aligned}
I^a(t+1) - I^a(t) &= I^{s_1}(t+1) - I^{s_1}(t) = I^{s_2}(t+1) - I^{s_2}(t) = 0 \\
I^{h_1}(t+1) - I^{h_1}(t) &= I^{h_2}(t+1) - I^{h_2}(t) = I^{h_3}(t+1) - I^{h_3}(t) = 0 \\
R(t+1) - R(t) &= 0.
\end{aligned}$$

The system (2) has two equilibrium points: the DFE and the endemic equilibrium. For strictly positive parameters, the DFE is given by

$$E_0 = \left(S^*, 0, \frac{\eta_1 S^*}{(\eta_2 + \gamma_0 + \mu)}, 0, 0, 0, 0, 0, \frac{\gamma_0 \eta_1 S^*}{(\theta + \mu)(\eta_2 + \gamma_0 + \mu)} \right), \quad (4)$$

with

$$S^* = \frac{(\theta + \mu)(\eta_2 + \gamma_0 + \mu)}{(\theta + \mu)(\eta_2 + \gamma_0 + \mu + \eta_1) + \eta_1 \gamma_0},$$

and the endemic equilibrium,

$$E_1 = \left(S^{**}, E^{**}, V^{**}, I^{a^{**}}, I^{s_1^{**}}, I^{s_2^{**}}, I^{h_1^{**}}, I^{h_2^{**}}, I^{h_3^{**}}, R^{**} \right) \quad (5)$$

exists if $R_v > 1$ with

$$\begin{aligned}
S^{**} &= \frac{1}{\alpha} \frac{K_1 K_3 K_4 K_5}{\beta_2 K_3 (K_5 + \lambda_1) + \beta_1 K_4 K_5}, \\
E^{**} &= \mu \frac{K_2 K_3 K_4 K_5 K_6 K_7 K_8 K_9}{K} \left(1 - \frac{1}{R_v} \right), \\
V^{**} &= \frac{1}{\alpha} \frac{\eta_1}{K_2} \frac{K_1 K_3 K_4 K_5}{\beta_2 K_3 (K_5 + \lambda_1) + \beta_1 K_4 K_5} \\
&\quad + \mu \left(\eta_3 + \frac{\eta_4 \beta_1}{K_3} \right) \frac{K_3 K_4 K_5 K_6 K_7 K_8 K_9}{K} \left(1 - \frac{1}{R_v} \right), \\
I^{a^{**}} &= \mu \beta_1 \frac{K_2 K_4 K_5 K_6 K_7 K_8 K_9}{K} \left(1 - \frac{1}{R_v} \right), \\
I^{s_1^{**}} &= \mu \beta_2 \frac{K_2 K_3 K_5 K_6 K_7 K_8 K_9}{K} \left(1 - \frac{1}{R_v} \right), \\
I^{s_2^{**}} &= \mu \lambda_1 \beta_2 \frac{K_2 K_3 K_6 K_7 K_8 K_9}{K} \left(1 - \frac{1}{R_v} \right), \\
I^{h_1^{**}} &= \mu \beta_3 \frac{K_2 K_3 K_4 K_5 K_7 K_8 K_9}{K} \left(1 - \frac{1}{R_v} \right), \\
I^{h_2^{**}} &= \mu \left(\frac{\lambda_2 \beta_3}{K_6} + \frac{\varphi \beta_2}{K_4} \right) \frac{K_2 K_3 K_4 K_5 K_6 K_8 K_9}{K} \left(1 - \frac{1}{R_v} \right), \\
I^{h_3^{**}} &= \mu \lambda_3 \left(\frac{\lambda_2 \beta_3}{K_6} + \frac{\varphi \beta_2}{K_4} \right) \frac{K_2 K_3 K_4 K_5 K_6 K_9}{K} \left(1 - \frac{1}{R_v} \right),
\end{aligned}$$

$$R^{**} = \frac{1}{\alpha} \frac{\gamma_0 \eta_1}{K_9 K_2} \frac{K_1 K_3 K_4 K_5}{\beta_2 K_3 (K_5 + \lambda_1) + \beta_1 K_4 K_5} + \mu \left(\frac{\gamma_0}{K_2} \left(\eta_3 + \frac{\eta_4 \beta_1}{K_3} \right) + \frac{\gamma_1 \beta_1}{K_3} + \frac{\gamma_2 \lambda_1 \beta_2}{K_5 K_4} \right) + \frac{\gamma_3}{K_7} \left(\frac{\lambda_2 \beta_3}{K_6} + \frac{\varphi \beta_2}{K_4} \right) + \frac{\gamma_4 \lambda_3}{K_8 K_7} \left(\frac{\lambda_2 \beta_3}{K_6} + \frac{\varphi \beta_2}{K_4} \right) \times \frac{K_2 K_3 K_4 K_5 K_6 K_7 K_8}{K} \left(1 - \frac{1}{R_v} \right),$$

and

$$\begin{cases} K_0 = (\eta_1 + \mu), \\ K_1 = (\beta_1 + \beta_2 + \beta_3 + \eta_3 + \mu), \\ K_2 = (\eta_2 + \gamma_0 + \mu), \\ K_3 = (\eta_4 + \gamma_1 + \mu), \\ K_4 = (\lambda_1 + \varphi + \mu), \end{cases} \quad \begin{cases} K_5 = (\gamma_2 + \mu), \\ K_6 = (\lambda_2 + \mu), \\ K_7 = (\lambda_3 + \gamma_3 + \delta_1 + \mu), \\ K_8 = (\gamma_4 + \delta_2 + \mu), \\ K_9 = (\theta + \mu), \end{cases} \quad (6)$$

$$K = \mu K_2 K_3 K_4 K_5 K_6 K_7 K_8 K_9 + \mu \eta_3 K_3 K_4 K_5 K_6 K_7 K_8 K_9 \quad (7) \\ + \mu \eta_3 \gamma_0 K_3 K_4 K_5 K_6 K_7 K_8 + \mu \gamma_4 \beta_2 \lambda_3 \varphi K_2 K_3 K_5 K_6 \\ + \mu \gamma_4 \lambda_2 \lambda_3 \beta_3 K_2 K_3 K_4 K_5 + \mu \beta_3 K_2 K_3 K_4 K_5 K_7 K_8 K_9 \\ + \mu \gamma_3 \lambda_2 \beta_3 K_2 K_3 K_4 K_5 K_8 + \mu \beta_2 K_2 K_3 K_5 K_6 K_7 K_8 K_9 \\ + \mu \lambda_1 \beta_2 K_2 K_3 K_6 K_7 K_8 K_9 + \mu \beta_1 \gamma_0 K_4 K_5 K_6 K_7 K_8 K_9 \\ + \mu \gamma_2 \lambda_1 \beta_2 K_2 K_3 K_6 K_7 K_8 + \mu \beta_1 \eta_2 K_4 K_5 K_6 K_7 K_8 K_9 \\ + \mu \gamma_1 \beta_1 \eta_2 K_4 K_5 K_6 K_7 K_8 + \mu \beta_1 \gamma_0 \eta_4 K_4 K_5 K_6 K_7 K_8 \\ + \mu \gamma_3 \beta_2 \varphi K_2 K_3 K_5 K_6 K_8 + \mu \beta_1 (\eta_4 + \mu) K_4 K_5 K_6 K_7 K_8 K_9 \\ + \mu \beta_1 \gamma_1 (\gamma_0 + \mu) K_4 K_5 K_6 K_7 K_8 + \lambda_2 \beta_3 (\delta_1 + \mu) K_2 K_3 K_4 K_5 K_8 K_9 \\ + \lambda_2 \lambda_3 \beta_3 (\delta_2 + \mu) K_2 K_3 K_4 K_5 K_9 + \varphi \beta_2 (\delta_1 + \mu) K_2 K_3 K_5 K_6 K_8 K_9 \\ + \lambda_3 \varphi \beta_2 (\delta_2 + \mu) K_2 K_3 K_5 K_6 K_9.$$

3 Stability analysis

In this section, we study the asymptotic stability of the equilibrium points of our system (2) in which the Jacobian matrix is given by

$$J(S_n, E_n, V_n, I_n^a, I_n^{s_1}, I_n^{s_2}, I_n^{h_1}, I_n^{h_2}, I_n^{h_3}, R_n) = (M_{i,j})_{i,j=1,10}$$

such as

$$\left\{ \begin{array}{l} M_{1,1} = -K_0 - \alpha(I_n^a + I_n^{s_1} + I_n^{s_2}), \\ M_{2,1} = \alpha(I_n^a + I_n^{s_1} + I_n^{s_2}), \\ M_{3,1} = \eta_1, \\ M_{2,2} = -K_1, \\ M_{3,2} = \eta_3, \\ M_{4,2} = \beta_1, \\ M_{5,2} = \beta_2, \\ M_{7,2} = \beta_3, \\ M_{1,3} = \eta_2, \\ M_{2,4} = M_{2,5} = M_{2,6} = \alpha S_n, \\ M_{1,4} = M_{1,5} = M_{1,6} = -\alpha S_n, \end{array} \right. \left\{ \begin{array}{l} M_{3,3} = -K_2, \\ M_{3,4} = \eta_4, \\ M_{4,4} = -K_3, \\ M_{10,3} = \gamma_0, \\ M_{5,5} = -K_4, \\ M_{6,5} = \lambda_1, \\ M_{10,4} = \gamma_1, \\ M_{6,6} = -K_5, \\ M_{8,5} = \varphi, \\ M_{7,7} = -K_6, \end{array} \right. \left\{ \begin{array}{l} M_{8,7} = \lambda_2, \\ M_{10,6} = \gamma_2, \\ M_{8,8} = -K_7, \\ M_{9,8} = \lambda_3, \\ M_{10,8} = \gamma_3, \\ M_{9,9} = -K_8, \\ M_{10,9} = \gamma_4, \\ M_{1,10} = \theta, \\ M_{10,10} = -K_9, \\ 0 \quad \text{otherwise,} \end{array} \right.$$

where $(K_i)_{i=0,\dots,9}$ are positive constants given in (6).

3.1 Asymptotic stability of DFE E_0

Theorem 1. The DFE of the system (2) is locally-asymptotically stable in Ω whenever $R_v \leq 1$.

Proof. The system (2) has a unique DFE described in (4).

The Jacobian matrix at E_0 is given by

$$J(E_0) = (M_{i,j})_{i,j=\overline{1,10}},$$

where

$$\left\{ \begin{array}{l} M_{1,1} = -K_0, \\ M_{3,1} = \eta_1, \\ M_{2,2} = -K_1, \\ M_{3,2} = \eta_3, \\ M_{4,2} = \beta_1, \\ M_{5,2} = \beta_2, \\ M_{7,2} = \beta_3, \\ M_{1,3} = \eta_2, \\ M_{1,4} = M_{1,5} = M_{1,6} = \frac{-\alpha K_9 K_2}{K_9 K_2 + \eta_1 K_9 + \eta_1 \gamma_0}, \\ M_{2,4} = M_{2,5} = M_{2,6} = \frac{\alpha K_9 K_2}{K_9 K_2 + \eta_1 K_9 + \eta_1 \gamma_0}, \end{array} \right. \quad \left\{ \begin{array}{l} M_{3,3} = -K_2, \\ M_{3,4} = \eta_4, \\ M_{4,4} = -K_3, \\ M_{10,3} = \gamma_0, \\ M_{5,5} = -K_4, \\ M_{6,5} = \lambda_1, \\ M_{10,4} = \gamma_1, \\ M_{6,6} = -K_5, \\ M_{8,5} = \varphi, \\ M_{7,7} = -K_6, \end{array} \right. \quad \left\{ \begin{array}{l} M_{8,7} = \lambda_2, \\ M_{10,6} = \gamma_2, \\ M_{8,8} = -K_7, \\ M_{9,8} = \lambda_3, \\ M_{10,8} = \gamma_3, \\ M_{9,9} = -K_8, \\ M_{10,9} = \gamma_4, \\ M_{1,10} = \theta, \\ M_{10,10} = -K_9, \\ 0 \quad \text{otherwise.} \end{array} \right.$$

The characteristic polynomial of $J(E_0)$ is given by,

$$P(X) = X^{10} + C_9 X^9 + C_8 X^8 + C_7 X^7 + C_6 X^6 + C_5 X^5 + C_4 X^4 + C_3 X^3 + C_2 X^2 + C_1 X + C_0.$$

If $R_v \leq 1$, then the coefficients $(C_i)_{i=0,9}$ are positives (Details are provided in Appendix 6). According to the criteria of Descartes, all eigenvalues of $J(E_0)$ are negative reals or complexes with negative real parts. Hence, E_0 is locally asymptotically stable in Ω . □

3.2 Asymptotic stability of the endemic equilibrium E_1

Theorem 2. The endemic equilibrium of our system (2), E_1 , is locally-asymptotically stable in Ω whenever $R_v > 1$.

Proof. The system (2) has a unique endemic equilibrium E_1 in Ω , given in 5.

The Jacobian matrix at E_1 is given by

$$J(E_1) = (M_{i,j})_{i,j=\overline{1,10}}$$

such as

$$\left\{ \begin{array}{l} M_{1,1} = -(K_0 + \alpha (I^{a^{**}} + I^{s_1^{**}} + I^{s_2^{**}})), \\ M_{2,1} = \alpha (I^{a^{**}} + I^{s_1^{**}} + I^{s_2^{**}}), \\ M_{3,1} = \eta_1, \\ M_{2,2} = -K_1, \\ M_{3,2} = \eta_3, \\ M_{4,2} = \beta_1, \\ M_{5,2} = \beta_2, \\ M_{7,2} = \beta_3, \\ M_{1,4} = M_{1,5} = M_{1,6} = -\alpha S^{**}, \\ M_{2,4} = M_{2,5} = M_{2,6} = \alpha S^{**}, \end{array} \right. \left\{ \begin{array}{l} M_{1,3} = \eta_2, \\ M_{3,3} = -K_2, \\ M_{3,4} = \eta_4, \\ M_{4,4} = -K_3, \\ M_{10,3} = \gamma_0, \\ M_{5,5} = -K_4, \\ M_{6,5} = \lambda_1, \\ M_{10,4} = \gamma_1, \\ M_{6,6} = -K_5, \\ M_{8,5} = \varphi, \\ M_{7,7} = -K_6, \end{array} \right. \left\{ \begin{array}{l} M_{8,7} = \lambda_2, \\ M_{10,6} = \gamma_2, \\ M_{8,8} = -K_7, \\ M_{9,8} = \lambda_3, \\ M_{10,8} = \gamma_3, \\ M_{9,9} = -K_8, \\ M_{10,9} = \gamma_4, \\ M_{1,10} = \theta, \\ M_{10,10} = -K_9, \\ 0 \text{ otherwise,} \end{array} \right.$$

where

$$\begin{aligned} S^{**} &= \frac{1}{\alpha} \frac{K_1 K_3 K_4 K_5}{\beta_2 K_3 (K_5 + \lambda_1) + \beta_1 K_4 K_5}, \\ I^{a^{**}} &= \mu \beta_1 \frac{K_2 K_4 K_5 K_6 K_7 K_8 K_9}{K} \left(1 - \frac{1}{R_v}\right), \\ I^{s_1^{**}} &= \mu \beta_2 \frac{K_2 K_3 K_5 K_6 K_7 K_8 K_9}{K} \left(1 - \frac{1}{R_v}\right), \\ I^{s_2^{**}} &= \mu \lambda_1 \beta_2 \frac{K_2 K_3 K_6 K_7 K_8 K_9}{K} \left(1 - \frac{1}{R_v}\right). \end{aligned}$$

The characteristic polynomial of $J(E_1)$ is given by

$$P(X) = X^{10} + C_9 X^9 + C_8 X^8 + C_7 X^7 + C_6 X^6 + C_5 X^5 + C_4 X^4 + C_3 X^3 + C_2 X^2 + C_1 X + C_0$$

If $R_v > 1$, then the coefficients $(C_i)_{i=0,9}$ are positives (Details are provided in Appendix 6). According to the criteria of Descartes, all eigenvalues of $J(E_1)$ are negative reals or complexes with negative real parts. Hence, E_1 is locally asymptotically stable in Ω . \square

4 Sensitivity analysis

To effectively reduce the transmission and prevalence of COVID-19, it is crucial to examine and understand the relative significance of various factors that contribute to their evolution. The vaccination reproduction number,

denoted as R_v , is a key parameter that directly affects disease transmission control. It measures the average number of cases an infected person generates during their infectious period in a population that is fully vaccinated. The long-term disease prevalence is represented by the endemic point E_1 . Conducting sensitivity analyses on these indicators can help identify the operational parameters that have a substantial impact on them [5, 20]. This knowledge can then be used to develop effective intervention strategies.

The normalized forward sensitivity index of a variable, f , that is differentially dependent on a parameter, x , is defined as:

$$\Upsilon_x^f = \frac{\partial f}{\partial x} \frac{x}{f}. \quad (8)$$

This section focuses on conducting local sensitivity analyses. Initially, sensitivity indices of R_v are calculated, followed by sensitivity indices of E_1 , using parameter values obtained from various sources listed in Table 3.

4.1 Sensitivity index of R_v

The formula for calculating R_v is explicitly given in (3). By using the analytical formulas provided in reference (8), sensitivity indices for R_v can be computed and presented in Table 1, using the parameter values from Table 3.

The sensitivity indices presented in Table 1 are sorted in descending order, indicating that the transmission rate α and the recovery rate of infected with moderate symptoms γ_2 are the most sensitive parameters. For instance, a 10% decrease (increase) in the transmission rate α results in a 10% decrease (increase) in R_v . Similarly, a 10% decrease (increase) in γ_2 leads to a 9.404% increase (decrease) in R_v . Therefore, it is crucial to accurately estimate these parameters, as even a small variation in them can cause significant quantitative changes. On the other hand, the lowest sensitive parameters, such as the recovery rate of vaccinated individuals γ_0 and the reinfection rate of vaccinated individuals η_2 , have a negligible effect on R_v . A 100% increase (or decrease) in γ_0 or η_2 leads to only a 0.047043% or 0.041779% increase (or decrease) in R_v , respectively.

Table 1: Sensitivity indices of R_v . The parameters are ordered from most sensitive to least

Parameters	Sensitivity index
α	1.0000
γ_2	-0.9404
β_2	0.6249
β_1	-0.6125
γ_1	-0.0225
λ_1	-0.0202
η_3	-0.0104
η_4	-0.0040
β_3	-0.0018
φ	-0.0018
η_1	-0.0017
θ	0.00066625
γ_0	0.00047043
η_2	0.00041779

4.2 Sensitivity index of E_1

The endemic equilibrium for the COVID-19 system (2), is given by (5). Using (8), the same approach can be followed to determine the sensitivity indices of each of the endemic equilibrium state variables.

Table 2 reveals that the most sensitive parameters for all infected states are the transition rates $(\lambda_i)_{i=1,2,3}$, rates at which exposed individuals become infected $(\beta_i)_{i=1,2,3}$, and recovery rates $(\gamma_i)_{i=1,2,3,4}$, respectively. Therefore, any variations in these parameters will significantly impact the proportion of infectious individuals. The reinfection rate θ is another parameter that strongly and positively affects the prevalence of COVID-19, and it is the most sensitive parameter for the recovery state. Increasing this parameter of 10 percent results in a decrease of 9,466 percent in the proportion of recovered individuals, leading to an increased risk of COVID-19 spread. Lastly, the parameters η_4 (vaccination rate of asymptotically infected individuals) and γ_2 (recovery rate of symptomatic infected) increase the proportion of

Table 2: Sensitivity indices of state variables at endemic equilibrium for baseline parameter values in Table 3

	S^{**}	E^{**}	V^{**}	I^a^{**}	$I^{s_1^{**}}$	$I^{s_2^{**}}$	$I^{H_1^{**}}$	$I^{H_2^{**}}$	$I^{H_3^{**}}$	R^{**}
α	-1	0.2800	0.2800	0.2800	0.2800	0.2800	0.2800	0.2800	0.2800	0.2734
β_1	0.6125	-0.2254	0.6763	0.7746	-0.2254	-0.2254	-0.2254	-0.2254	-0.2254	0.4102
β_2	-0.6249	-0.7206	-0.7206	-0.7206	0.2794	-0.7206	-0.7206	-0.4531	-0.4531	-0.3663
β_3	0.0018	-0.0069	-0.0069	-0.0069	-0.0069	0.9931	0.9931	0.7256	0.7256	-0.0051
η_1	0	0.0047	-0.000468	-0.000468	-0.000468	-0.000468	-0.000468	-0.000468	-0.000468	0.0047
η_2	0	-0.0198	-0.2479	0.0020	0.0020	0.0020	0.0020	0.0020	0.0020	-0.0198
η_3	0.0104	0.0045	0.0946	-0.0036	-0.0036	-0.0036	-0.0036	-0.0036	-0.0036	0.0045
η_4	0.0040	-0.0206	0.7669	-0.1495	0.000301	0.000301	0.000301	0.000301	0.000301	-0.0206
γ_0	0	0.0022	-0.7478	0.0022	0.0022	0.0022	0.0022	0.0022	0.0022	0.0239
γ_1	0.0225	0.0159	-0.7506	-0.8341	0.0159	0.0159	0.0159	0.0159	0.0159	0.0369
γ_2	0.9404	0.5741	0.5741	0.5741	-0.4145	-0.4145	0.5741	0.5741	0.5741	0.5800
γ_3	0	0.0036	0.0036	0.0036	0.0036	0.0036	0.0036	-0.7376	-0.7376	0.0034
γ_4	0	0.0025	0.0025	0.0025	0.0025	0.0025	0.0025	0.0025	-0.9775	0.0025
λ_1	0.0202	0.0146	0.0146	0.0146	-0.9833	0.0146	0.0146	-0.2523	-0.2523	0.0146
λ_2	0	0.000061	0.000061	0.000061	1.0001	-0.9998	-0.9998	0.000188	0.000188	0.000061
λ_3	0	0.0024	0.0024	0.0024	0.0024	0.0024	0.0024	-0.2445	0.7555	0.0025
δ_1	0	-0.0058	-0.0058	-0.0058	-0.0058	-0.0058	-0.0058	-0.0177	-0.0177	-0.0058
δ_2	0	-0.0025	-0.0025	-0.0025	-0.0025	-0.0025	-0.0025	-0.0025	-0.0223	-0.0025
θ	0	0.0535	0.0535	0.0535	0.0535	0.0535	0.0535	0.0535	0.0535	-0.9466
φ	0.0018	-0.0010	-0.0012	-0.0012	-0.0031	-0.0031	-0.0012	0.2658	0.2658	-0.0010

vaccinated individuals. Therefore, the population becomes immune to the disease, ultimately leading to the eradication of COVID-19.

5 Numerical simulation

This section aims to provide numerical simulations of the proposed model to demonstrate its practicality and effectiveness, and to illustrate our theoretical findings. The operational parameters used in the simulations are in Table 3.

Given that the model is discrete, the transitions between compartments are governed by the following rules:

- For the compartment of exposed individuals, those with a negative test result who will be vaccinated are represented by η_3 , while the rest of the exposed individuals are divided into asymptomatic ($\beta_1 = 0.55 \times (1 - \eta_3 - \mu)$), symptomatic ($\beta_2 = 0.30 \times (1 - \eta_3 - \mu)$), and hospitalized ($\beta_3 = 0.15 \times (1 - \eta_3 - \mu)$) individuals, according to [18].

Table 3: The values of operational parameters per week

Parameters	Description	Range of values	Source
α	Transmission rate.	0.002-0.2	[7,14]
β_1	Asymptomatic infection rate among exposed.	0.4-0.55	[7,14]
β_2	Rate of infection with symptoms among exposed.	0.2-0.3	[7,14]
β_3	Rate of hospitalization among exposed individuals.	0.001-0.15	[7,14]
η_1	Vaccination rate of susceptible individuals.	0.00001-0.2	[7,14]
η_2	Co-infection rate of vaccinated individuals.	0.2-0.35	[7,14]
η_3	Vaccination rate of exposed individuals.	0.0001-0.2	[7,14]
η_4	Vaccination rate of asymptotically infected.	0.1-0.55	[7,14]
γ_0	Recovery rate of vaccinated individuals.	0.65-0.75	[7,14]
γ_1	Recovery rate of asymptomatic infected.	0.45-0.85	[7,14]
γ_2	Recovery rate of symptomatic infected.	0.015-1.0	[7,14]
γ_3	Recovery rate of hospitalized infected in 2 nd phase.	0.2-0.75	[7,14]
γ_4	Recovery rate of hospitalized infected in 3 rd phase.	0.95-0.98	[7,14]
λ_1	Evolution rate symptomatic phase 1 to 2.	0.6-0.7	[7,14]
λ_2	Evolution rate hospitalized phase 1 to 2.	0.95-1.0	[7,14]
λ_3	Evolution rate hospitalized phase 2 to 3.	0.2-0.8	[7,14]
δ_1	Hospitalized COVID-19 mortality, phase 2.	0.01-0.02	[3,7,14]
δ_2	Hospitalized COVID-19 mortality, phase 3.	0.015-0.05	[3,7,14]
θ	Coinfection rate of recovery individuals	0.55-0.85	[7,14]
φ	The hospitalization rate of symptomatic in phase 1.	0.001-0.35	[3,7,14]
μ	Natural mortality rate	0.0001-0.002	[7,14]

- The efficacy of the vaccine is represented by γ_0 in the compartment of vaccinated individuals, with $\eta_2 = (1 - \gamma_0 - \mu)$ representing the proportion of vaccinated individuals who are not protected by the vaccine.
- In the compartment of asymptomatic infected individuals, the recovery rate is represented by γ_1 , and $\eta_4 = (1 - \gamma_1 - \mu)$ represents the proportion of asymptomatic infected individuals who will be vaccinated.
- For the compartment of symptomatic infected individuals not requiring hospitalization, the proportion of individuals entering the second week of illness is represented by λ_1 , while $\varphi = (1 - \lambda_1 - \mu)$ represents the proportion of individuals whose condition worsens and requires hospitalization.

- In the compartment of hospitalized infected individuals in the second phase, the recovery rate is represented by γ_3 , λ_3 represents the proportion of individuals who remain hospitalized, and the mortality rate due to COVID-19 is represented by $\delta_1 = 1 - \gamma_3 - \lambda_3 - \mu$.
- Finally, in the compartment of hospitalized infected individuals in the final phase, the recovery rate is represented by γ_4 , and the mortality rate due to COVID-19 is represented by $\delta_2 = 1 - \gamma_4 - \mu$.

5.1 Numerical stability

In this subsection, we verify the theoretical results obtained above through numerical simulations.

1. The following parameter values (per week) are used:

$$\begin{aligned} \alpha = 0.0025, \quad \gamma_0 = 0.65, \quad \gamma_1 = 0.45, \quad \gamma_3 = 0.2, \\ \gamma_4 = 0.95, \quad \eta_1 = 0.2, \quad \eta_3 = 0.2, \quad \theta = 0.55, \quad \lambda_3 = 0.78. \end{aligned} \quad (9)$$

The existence and stability conditions in theorem 1 are satisfied,

$$R_v = 0.0015 < 1.$$

Therefore, the system (2) has a DFE in Ω ,

$$E_0 = (0.6962, 0, 0.1392, 0, 0, 0, 0, 0, 0.1645).$$

Figure 2 indicates under some conditions that the long-term behavior of the solution curves of the system approaches the free equilibrium E_0 , as revealed by numerical simulations. This suggests that the population under consideration gradually becomes free of the infection.

Based on the numerical simulations depicted in Figure 2, it can be observed that the behavior of the solution curves of the system approaches the DFE E_0 over a long period of time. This simulation confirms the theoretical results outlined in section 3.

2. The following parameter values (per week) are used:

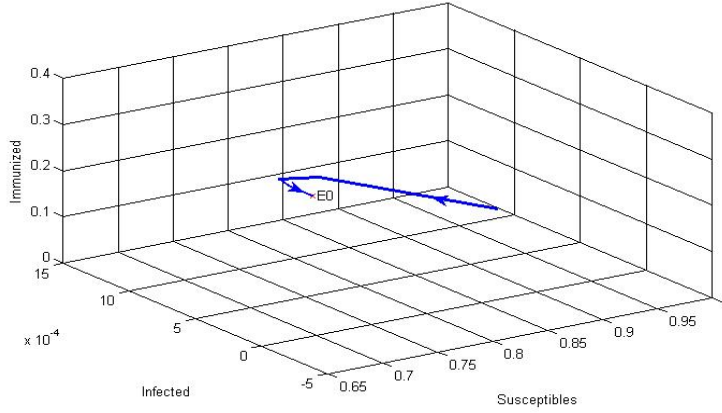


Figure 2: The proposed model has only one DFE E_0 , which is asymptotically stable when $R_v \leq 1$.

$$\alpha = 0.19, \quad \gamma_0 = 0.75, \quad \gamma_1 = 0.85, \quad \gamma_3 = 0.75, \quad \gamma_4 = 0.98, \tag{10}$$

$$\eta_1 = 0.00089, \quad \eta_3 = 0.0089, \quad \theta = 0.85, \quad \lambda_3 = 0.24.$$

The existence and stability conditions in Theorem 2 are satisfied,

$$R_v = 4.5711 > 1.$$

There is only one endemic equilibrium point in Ω ,

$$E_1 = \left(0.21840, \quad 0.03385, \quad 0.00326, \quad 0.018451, \quad 0.015451, \right. \\ \left. 0.661920, \quad 0.0000507, \quad 0.000068, \quad 0.000017, \quad 0.033088 \right).$$

Numerical simulations in Figure 3 demonstrate that the solution curves of the system approach the endemic equilibrium E_1 over an extended period.

Our proposed discrete model for coronavirus disease 2019 underwent numerical processing, which confirmed the existence of two equilibrium points. The first is the DFE E_0 , which is locally asymptotically stable when $R_v \leq 1$.

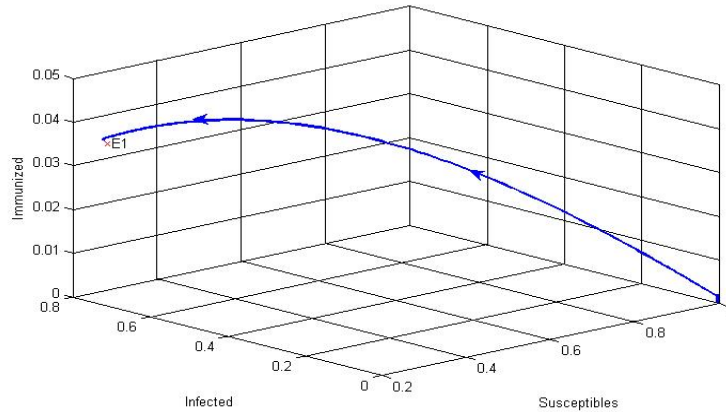


Figure 3: The proposed model has only one endemic equilibrium E_1 , which is asymptotically stable when $R_v > 1$.

The second is the endemic equilibrium E_1 , which is locally asymptotically stable when $R_v > 1$.

5.2 The effect of the most sensitive parameters of the model

It is important to note that the transmission rate α is mainly influenced by non-pharmaceutical measures such as physical distancing, the use of masks, quarantine and isolation of infected or exposed individuals, as well as limitations on nonessential gatherings and travel. Medical care is also an important factor that can impact the recovery rate γ_0 , γ_1 , γ_3 , and γ_4 for COVID-19. This includes access to appropriate medical facilities, equipment, and trained health-care professionals. The availability of treatments and medications that can effectively manage COVID-19 symptoms can also impact the recovery rate by reducing the duration and severity of the illness.

The primary objective of the simulations was to observe how the model parameters most affected the transmission dynamics and spread of COVID-19. Table 3 values were used in conjunction with varying levels of α , γ_0 , γ_1 ,

γ_3 , and γ_4 , which were increased in stages, ranging from mild to moderate and strict rates. The results of the simulations provide insight into the impact of control measures on the spread of the disease. By analyzing the effects of different levels, policymakers and public health officials can make informed decisions regarding the implementation of measures to curb the spread of COVID-19.

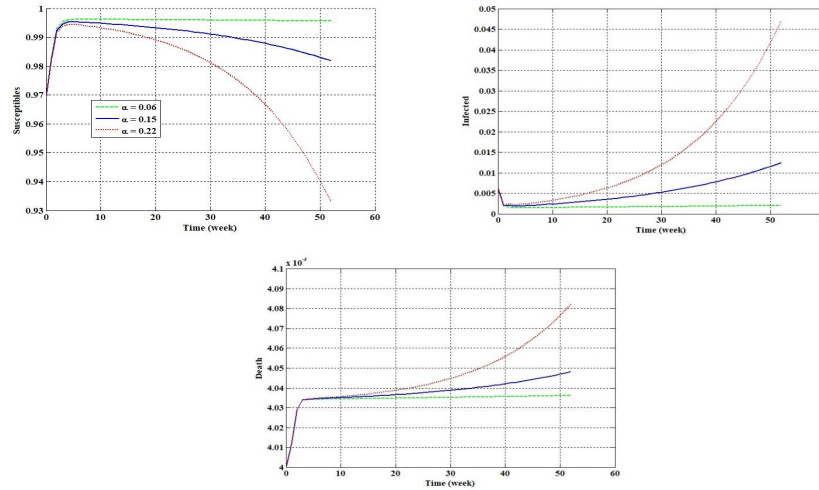


Figure 4: Effect of α transmission rate on different states of COVID-19.

Figures 4 and 5 present the results of numerical simulations conducted to investigate the effects of model parameters on the transmission dynamics and spread of COVID-19. The simulations were performed using different values of α , γ_0 , γ_1 , γ_3 , and γ_4 , and the results provide valuable insights into the impact of control measures on the spread of the disease.

Figure 4 shows that the rate of transmission is a critical factor in determining the number of people infected with COVID-19. The graph indicates that the higher the transmission rate α , the greater the number of infected individuals. When the transmission rate increases from the lowest 0.06 to the highest 0.22, the number of infections increases by more than 4 percent, as well as the COVID-19 mortality increases by $0.047e - 2$ percent. This finding highlights the importance of implementing effective measures to control the

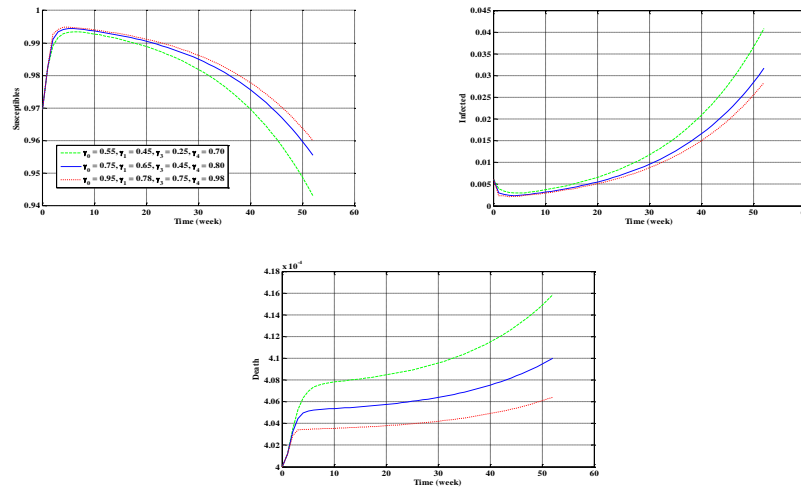


Figure 5: Effective recovery rates $\gamma_0, \gamma_1, \gamma_3,$ and γ_4 on the number of COVID-19 infected cases.

spread of the virus, such as social distancing, wearing masks, and limiting large gatherings.

Figure 5 examines the impact of the recovery rates $\gamma_0, \gamma_1, \gamma_3,$ and γ_4 on the number of infections. The graph shows that increasing the recovery rates results in a reduction in the number of infections. However, the effect of $\gamma_0, \gamma_1, \gamma_3,$ and γ_4 is less pronounced than that of α . When the values of $\gamma_0, \gamma_1, \gamma_3,$ and γ_4 are changed from the highest to the lowest, the difference in the number of infections is around 1.5 percent, as well as the mortality from COVID-19 decreases by $0.10e - 2$ percent. This finding suggests that while recovery rates are essential in reducing the spread of the disease, they may not be sufficient on their own. A combination of measures, including vaccination, testing, and contact tracing, may be necessary to achieve effective control of the virus.

The results presented in Figures 4 and 5 are consistent with the sensitivity analysis results obtained earlier. The sensitivity analysis revealed that the transmission rate α had a significant impact on the number of infections, while the recovery rates $\gamma_0, \gamma_1, \gamma_3,$ and γ_4 had a smaller effect. The simula-

tions conducted in Figures 4 and 5 confirm these findings and provide further evidence of the importance of controlling the transmission rate.

Overall, the numerical simulations provide important insights into the transmission dynamics and spread of COVID-19. By varying the values of α , γ_0 , γ_1 , γ_3 , and γ_4 , the simulations show how different control measures can affect the spread of the virus. The results indicate that while recovery rates are important in reducing the number of infections, the transmission rate is the primary determinant of the spread of the disease.

In conclusion, the numerical simulations presented in Figures 4 and 5 provide valuable insights into the transmission dynamics and spread of COVID-19. The simulations confirm the importance of controlling the transmission rate and suggest that recovery rates alone may not be sufficient in reducing the spread of the virus. The findings of the simulations can inform the development of effective control measures to curb the spread of COVID-19 and help mitigate the impact of the pandemic on public health and the economy.

6 Conclusion

In this research, we have conducted a comprehensive analysis of the factors affecting the transmission dynamics of COVID-19, employing both sensitivity analysis and numerical simulations. Our results shed light on the fundamental mechanisms governing the spread of the virus, offering critical insights for pandemic management and public health policy.

Sensitivity analysis revealed that the transmission rate α and the recovery rate of individuals with moderate symptoms (γ_2) are highly influential parameters. Small changes in these values can result in substantial alterations in the course of the pandemic. This underscores the imperative of precise parameter estimation and the significance of control measures that directly impact these variables.

Furthermore, numerical simulations provided a practical perspective, reinforcing the pivotal role of the transmission rate. The simulations demonstrated that variations in α have a profound effect on the number of infections and, subsequently, the COVID-19 mortality rate. This underscores the importance of strict public health interventions such as social distancing, mask-

wearing, and restrictions on gatherings to control viral transmission. While the recovery rates γ_0 , γ_1 , γ_3 , and γ_4 also play a role in reducing infections, their impact is less pronounced compared to α . This suggests that a multi-faceted approach, encompassing vaccination, testing, and contact tracing, is essential to effectively manage the pandemic.

In sum, our study emphasizes the critical need for tailored public health strategies, underpinned by a thorough understanding of the varying impacts of different parameters. These findings are pertinent to real-world policy decisions, guiding efforts to mitigate the consequences of the COVID-19 pandemic on both public health and the economy.

Appendix

The following calculations were performed using the mathematical software (Maxima Version 5.42.1).

The characteristic polynomial of $J(E_0)$ is given by

$$P(X) = X^{10} + C_9X^9 + C_8X^8 + C_7X^7 + C_6X^6 + C_5X^5 + C_4X^4 + C_3X^3 + C_2X^2 + C_1X + C_0.$$

So we have

$$\eta_1\eta_2 < (\eta_1 + \mu)(\eta_2 + \gamma_0 + \mu) < K_0K_2, \quad (11)$$

$$\begin{aligned} & \alpha S^* (\beta_1 (K_4 + K_5) + \beta_2 (K_3 + K_5) + \lambda_1 \beta_2) \quad (12) \\ &= \alpha S^* \left(\beta_1 K_4 K_5 \left(\frac{1}{K_4} + \frac{1}{K_5} \right) + \beta_2 K_3 K_5 \left(\frac{1}{K_3} + \frac{1}{K_5} \right) + \lambda_1 \beta_2 K_3 \frac{1}{K_3} \right) \\ &< \alpha S^* (\beta_1 K_4 K_5 + \beta_2 K_3 K_5 + \lambda_1 \beta_2 K_3) \left(\frac{1}{K_3} + \frac{1}{K_4} + \frac{1}{K_5} \right) \\ &< K_1 K_3 K_4 K_5 R_v \left(\frac{1}{K_3} + \frac{1}{K_4} + \frac{1}{K_5} \right) \\ &< (K_1 K_3 K_4 + K_1 K_3 K_5 + K_1 K_4 K_5) R_v, \end{aligned}$$

and

$$\begin{aligned}
\alpha S^* (\beta_1 + \beta_2) &= \alpha S^* \left(\beta_1 K_4 K_5 \frac{1}{K_4 K_5} + \beta_2 K_3 K_5 \frac{1}{K_3 K_5} \right) \quad (13) \\
&< \alpha S^* (\beta_1 K_4 K_5 + \beta_2 K_3 K_5 + \lambda_1 \beta_2 K_3) \left(\frac{1}{K_4 K_5} + \frac{1}{K_3 K_5} \right) \\
&< K_1 K_3 K_4 K_5 R_v \left(\frac{1}{K_4 K_5} + \frac{1}{K_3 K_5} \right) \\
&< (K_1 K_3 + K_1 K_4) R_v.
\end{aligned}$$

We pose

$$\begin{cases} \mathbf{P}_1 = K_0 K_2 - \eta_1 \eta_2, \\ \mathbf{P}_2 = (K_1 K_3 K_4 + K_1 K_3 K_5 + K_1 K_4 K_5) \\ \quad - \alpha S^* (\beta_1 (K_4 + K_5) + \beta_2 (K_3 + K_5 + \lambda_1)), \\ \mathbf{P}_3 = (K_1 K_3 + K_1 K_4) - \alpha S^* (\beta_1 + \beta_2). \end{cases}$$

The coefficients of the characteristic polynomial are given by

$$C_0 = \frac{\mu}{S^*} K_1 K_2 K_3 K_4 K_5 K_6 K_7 K_8 K_9 (1 - R_v),$$

$$\begin{aligned}
C_1 &= \frac{\mu}{S^*} K_2 K_6 K_7 K_8 K_9 (K_3 K_4 K_5 + \mathbf{P}_2) \\
&\quad + K_1 K_3 K_4 K_5 K_6 K_7 K_8 (K_0 K_9 + K_2 K_9 + \mathbf{P}_1) (1 - R_v) \\
&\quad + \frac{\mu}{S^*} K_1 K_2 K_3 K_4 K_5 K_9 (K_6 K_7 + K_6 K_8 + K_7 K_8) (1 - R_v),
\end{aligned}$$

$$\begin{aligned}
C_2 &= K_6 K_7 K_8 K_9 (K_1 K_3 K_4 + K_1 K_3 K_5 + K_1 K_4 K_5 + K_3 K_4 K_5) (K_0 + K_2) \\
&\quad + K_1 K_3 K_4 K_5 K_8 K_9 (K_6 K_7 + K_2 K_7 + K_0 K_7 + K_0 K_6 + K_2 K_6) (1 - R_v) \\
&\quad + K_1 K_3 K_4 K_5 K_6 K_7 (K_0 K_9 + K_2 K_9 + K_0 K_8 + K_2 K_8) (1 - R_v) \\
&\quad + \frac{\mu}{S^*} K_1 K_2 K_3 K_4 K_5 K_9 (K_6 + K_7 + K_8) (1 - R_v) + K_6 K_7 K_8 \mathbf{P}_1 \mathbf{P}_2 \\
&\quad + \frac{\mu}{S^*} K_2 K_9 (K_1 K_5 K_6 K_7 K_8 + K_3 K_5 K_6 K_7 K_8 + K_4 K_5 K_6 K_7 K_8) \\
&\quad + \frac{\mu}{S^*} K_2 K_3 K_4 K_9 (K_5 K_6 K_7 + K_5 K_6 K_8 + K_5 K_7 K_8 + K_6 K_7 K_8) \\
&\quad + \frac{\mu}{S^*} K_2 K_9 (K_6 K_7 + K_6 K_8 + K_7 K_8) \mathbf{P}_2 + K_6 K_7 K_8 K_9 (K_0 + K_2) \mathbf{P}_2 \\
&\quad + K_1 K_3 K_4 K_5 (K_6 K_7 + K_6 K_8 + K_8 K_7) \mathbf{P}_1 (1 - R_v) \\
&\quad + K_3 K_4 K_5 K_6 K_7 K_8 \mathbf{P}_1 + \frac{\mu}{S^*} K_2 K_6 K_7 K_8 K_9 \mathbf{P}_3,
\end{aligned}$$

$$\begin{aligned}
C_3 = & K_1 K_3 K_4 K_5 \left(K_6 K_7 (K_8 + K_9) + (K_6 + K_7) K_8 K_9 + \frac{\mu}{S^*} K_2 K_9 \right) (1 - R_v) \\
& + K_5 K_6 K_7 K_8 K_9 ((K_1 + K_3 + K_4) (K_0 + K_2) + K_3 K_4) + K_6 K_7 K_8 \mathbf{P}_3 \mathbf{P}_1 \\
& + K_1 K_3 K_4 K_5 (K_8 (K_7 + K_6 + K_9) + (K_7 + K_6) K_9) (K_0 + K_2) (1 - R_v) \\
& + K_3 K_4 K_5 K_6 K_8 K_9 (K_0 + K_2) + K_1 K_3 K_4 K_5 K_6 K_7 (K_0 + K_2) (1 - R_v) \\
& + K_3 K_4 (K_7 K_8 (K_6 K_9 + K_5 K_9) + K_6 K_7 (K_5 K_9 + K_5 K_8)) (K_0 + K_2) \\
& + \frac{\mu}{S^*} K_2 K_9 (K_1 K_5 K_6 K_8 + K_3 K_4 K_5 K_8 + K_1 K_5 K_7 K_8 + K_3 K_4 K_6 K_8) \\
& + \frac{\mu}{S^*} K_2 K_9 (K_7 K_8 + K_6 K_8 + K_7 K_6) \mathbf{P}_3 + K_6 K_7 K_8 K_9 (K_0 + K_2) \mathbf{P}_3 \\
& + \frac{\mu}{S^*} K_2 K_9 (K_7 K_8 (K_1 K_6 + K_3 K_4 + K_3 K_5) + K_5 K_6 K_8 (K_3 + K_4)) \\
& + \frac{\mu}{S^*} K_2 K_9 (K_6 K_7 K_8 (K_3 + K_4 + K_5) + K_4 K_5 K_7 K_8 + K_3 K_4 K_5 K_6) \\
& + \frac{\mu}{S^*} K_2 K_9 (K_5 K_6 K_7 (K_1 + K_3 + K_4) + K_3 K_4 K_5 K_7 + K_3 K_4 K_6 K_7) \\
& + \frac{\mu}{S^*} K_2 K_9 (K_8 + K_7 + K_6) \mathbf{P}_2 + K_1 K_3 K_4 K_5 (K_8 + K_7 + K_6) \mathbf{P}_1 (1 - R_v) \\
& + (K_0 K_7 (K_6 K_8 + K_6 K_9 + K_8 K_9) + K_0 K_6 K_8 K_9 + K_2 K_6 K_7 (K_8 + K_9)) \mathbf{P}_2 \\
& + (K_7 K_8 + K_6 K_8 + K_6 K_7) \mathbf{P}_1 \mathbf{P}_2 + K_8 K_9 (K_2 K_6 + K_2 K_7 + K_6 K_7) \mathbf{P}_2 \\
& + K_5 K_6 K_7 K_8 (K_3 + K_4 + K_1) \mathbf{P}_1 + K_7 K_3 K_4 (K_5 K_6 + K_5 K_8 + K_6 K_8) \mathbf{P}_{1,1}
\end{aligned}$$

$$\begin{aligned}
C_4 = & K_3 K_9 (K_7 K_8 (K_6 + K_5 + K_4) + K_8 (K_5 K_6 + K_4 K_6 + K_5 K_4)) (K_0 + K_2) \\
& + K_4 (K_8 K_9 (K_6 K_7 + K_5 K_7 + K_5 K_6) + K_5 K_6 K_7 (K_9 + K_8)) (K_0 + K_2) \\
& + K_3 (K_6 K_7 (K_5 K_8 + K_4 K_8 + K_4 K_5) + K_4 K_5 K_8 (K_7 + K_6)) (K_0 + K_2) \\
& + K_1 (K_8 K_9 (K_6 K_7 + K_5 K_7 + K_5 K_6) + K_5 K_6 K_7 (K_9 + K_8)) (K_2 + K_0) \\
& + \frac{\mu}{S^*} K_2 K_9 K_8 K_7 (K_6 + K_5 + K_4 + K_3 + K_1) + K_1 K_3 K_4 K_5 (1 - R_v) \mathbf{P}_1 \\
& + K_1 K_3 K_4 K_5 ((K_8 + K_7 + K_6) K_9 + (K_7 + K_6) K_8 + K_6 K_7) (1 - R_v) \\
& + K_7 K_8 K_9 (K_1 K_5 K_6 + K_3 K_5 K_6 + K_4 K_5 K_6 + K_3 K_4 K_5 + K_3 K_4 K_6) \\
& + K_3 K_4 K_5 K_6 (K_7 K_8 + K_7 K_9 + K_8 K_9) + K_5 K_6 K_7 K_8 K_9 (K_0 + K_2) \\
& + K_3 K_9 (K_5 K_6 K_7 + K_4 K_6 K_7 + K_5 K_4 K_7 + K_6 K_5 K_4) (K_0 + K_2) \\
& + \frac{\mu}{S^*} K_2 K_9 K_6 (K_8 + K_7) (K_5 + K_4 + K_3 + K_1) + K_6 K_7 K_8 K_9 \mathbf{P}_3 \\
& + K_9 ((K_7 K_8 + K_6 K_8 + K_6 K_7) + (K_8 + K_7 + K_6) (K_0 + K_2)) \mathbf{P}_2 \\
& + (K_8 + K_7 + K_6) \mathbf{P}_1 \mathbf{P}_2 + \frac{\mu}{S^*} K_2 K_3 K_4 K_9 (K_5 + K_6 + K_7 + K_8) \\
& + (K_7 K_8 + K_6 K_8 + K_6 K_7) \mathbf{P}_1 \mathbf{P}_3 + K_3 K_4 K_5 (K_8 + K_7 + K_6) \mathbf{P}_1
\end{aligned}$$

$$\begin{aligned}
& + (K_7K_8K_9 + K_6K_8K_9 + K_6K_7K_9 + K_8K_7K_6) (K_2 + K_0) \mathbf{P}_3 \\
& + K_6K_8 (K_1K_5 + K_3K_4 + K_4K_5 + K_3K_7 + K_1K_7 + K_3K_5) \mathbf{P}_1 \\
& + K_7K_8 (K_3K_4 + K_1K_5 + K_4K_5 + K_4K_6 + K_5K_6 + K_3K_5) \mathbf{P}_1 \\
& + K_6K_7 (K_1K_5 + K_4K_5 + K_3K_4 + K_3K_5) \mathbf{P}_1 + \frac{\mu}{S^*} K_2K_9\mathbf{P}_2 \\
& + \frac{\mu}{S^*} K_2K_9 (K_6 + K_7 + K_8) (K_5 (K_1 + K_3 + K_4) + \mathbf{P}_3) \\
& + K_1K_3K_4K_5 (K_8 + K_7 + K_9 + K_6) (K_0 + K_2) (1 - R_v) \\
& + (K_6K_7K_8 + (K_7K_8 + K_6K_8 + K_7K_6) (K_0 + K_2)) \mathbf{P}_2,
\end{aligned}$$

$$\begin{aligned}
C_5 = & K_3 (K_0 + K_2) (K_7K_6K_8 + (K_7K_8 + K_6K_8 + K_7K_6) (K_5 + K_4)) \\
& + K_5 (K_0 + K_1 + K_2 + K_3 + K_4) (K_9 (K_8 (K_7 + K_6) + K_7K_6)) \\
& + K_4K_9 (K_0 + K_2 + K_3) (K_8 (K_7 + K_6 + K_5) + K_7 (K_6 + K_5)) \\
& + K_4 (K_0 + K_2 + K_3) (K_8 (K_7 (K_5 + K_6) + K_6K_5) + K_7K_6K_5) \\
& + K_3K_4K_5 (K_0 + K_2) (K_8 + K_7 + K_6) + (K_8 + K_7 + K_6) \mathbf{P}_1\mathbf{P}_3 \\
& + ((K_7K_8 + K_6K_8 + K_6K_7) K_9 + K_7K_8K_6) \mathbf{P}_3 + \frac{\mu}{S^*} K_2K_9\mathbf{P}_3 \\
& + (K_7K_8 + K_6K_8 + K_9 (K_8 + K_7 + K_6) + K_7K_6) (K_0 + K_2) \mathbf{P}_3 \\
& + K_1K_3K_4K_5 (K_9 + K_8 + K_7 + K_6 + K_2 + K_0) (1 - R_v) + \mathbf{P}_2\mathbf{P}_1 \\
& + \frac{\mu}{S^*} K_2K_9 (K_6 (K_1 + K_3 + K_4 + K_5) + K_5 (K_1 + K_3 + K_4)) \\
& + ((K_7 + K_6) K_8 + (K_6 + K_7 + K_8 + K_9) (K_0 + K_2) + K_7K_6) \mathbf{P}_2 \\
& + K_3K_9 (K_0 + K_2) (K_8 (K_7 + K_6) + (K_8 + K_7 + K_6) (K_5 + K_4)) \\
& + ((K_8 + K_7 + K_6) K_9) \mathbf{P}_2 + K_3K_9 (K_0 + K_2) (K_7K_6 + K_5K_4) \\
& + K_7 \left(\frac{\mu}{S^*} K_2K_9 + K_8\mathbf{P}_1 \right) (K_1 + K_3 + K_4 + K_5 + K_6) \\
& + K_1 (K_2 + K_0) (K_7K_8K_9 + K_6K_5 (K_9 + K_8 + K_7)) \\
& + K_1 (K_2 + K_0) (K_8K_9 + K_7K_9 + K_7K_8) (K_6 + K_5) \\
& + \frac{\mu}{S^*} K_2K_9 (K_8 (K_1 + K_3 + K_4 + K_5 + K_6 + K_7)) \\
& + \frac{\mu}{S^*} K_2K_3K_4K_9 + K_4K_5K_6K_9 (K_0 + K_2 + K_3) \\
& + K_9K_8K_7K_6 (K_0 + K_1 + K_2 + K_3 + K_4 + K_5) \\
& + (K_6K_8 + K_6K_7) (K_1 + K_3 + K_4 + K_5) \mathbf{P}_1
\end{aligned}$$

$$\begin{aligned}
& + K_5 K_6 K_7 K_8 (K_0 + K_1 + K_2 + K_3 + K_4) \\
& + K_3 K_4 (K_5 + K_6 + K_7 + K_8) \mathbf{P}_1 \\
& + (K_5 (K_7 + K_6 + K_8) (K_1 + K_3 + K_4)) \mathbf{P}_1,
\end{aligned}$$

$$\begin{aligned}
C_6 = & (K_8 (K_7 + K_6 + K_5 + K_4 + K_3 + K_1) + K_7 (K_6 + K_5 + K_4 + K_3 + K_1)) \mathbf{P}_1 \\
& + (K_5 (K_0 + K_1 + K_2 + K_3 + K_4) + K_3 (K_2 + K_0)) (K_8 (K_7 + K_6) + K_7 K_6) \\
& + K_2 K_1 (K_9 (K_8 + K_7 + K_6 + K_5) + K_8 (K_7 + K_6 + K_5) + K_7 (K_6 + K_5)) \\
& + \frac{\mu}{S^*} K_2 K_9 (K_1 + K_3 + K_4 + K_5 + K_6 + K_7 + K_8) + K_1 K_3 K_4 K_5 (1 - R_v) \\
& + K_4 (K_0 + K_2 + K_3) (K_9 (K_8 + K_7 + K_6 + K_5) + K_8 (K_7 + K_6 + K_5)) \\
& + K_9 (K_5 (K_0 + K_1 + K_2 + K_3 + K_4) + K_3 (K_2 + K_0)) (K_8 + K_7 + K_6) \\
& + K_7 (K_0 K_1 + K_4 K_3) (K_6 + K_5) + K_4 K_6 K_7 (K_0 + K_2) + K_4 K_3 K_6 K_5 \\
& + (K_9 (K_8 + K_7 + K_6) + K_6 K_7 + (K_9 + K_8 + K_7 + K_6) (K_0 + K_2)) \mathbf{P}_3 \\
& + (K_3 K_4 (K_5 + K_6 + K_7 + K_8 + K_9) + K_4 K_5 (K_6 + K_7)) (K_0 + K_2) \\
& + K_0 K_1 (K_9 (K_8 + K_7 + K_6 + K_5) + K_8 (K_7 + K_6 + K_5) + K_6 K_5) \\
& + K_7 K_8 K_9 (K_0 + K_1 + K_2 + K_3 + K_4 + K_5 + K_6) + K_1 K_2 K_5 K_6 \\
& + K_6 (K_0 + K_1 + K_2 + K_3 + K_4 + K_5) (K_9 (K_8 + K_7) + K_8 K_7) \\
& + (K_6 (K_5 + K_4 + K_3 + K_1) + K_5 (K_4 + K_3 + K_1) + K_4 K_3) \mathbf{P}_1 \\
& + K_3 K_5 (K_6 + K_7 + K_8 + K_9) (K_0 + K_2) + K_8 (K_7 + K_6) \mathbf{P}_3 \\
& + (K_9 + K_8 + K_7 + K_6 + K_2 + K_0) \mathbf{P}_2 + \mathbf{P}_3 \mathbf{P}_1,
\end{aligned}$$

$$\begin{aligned}
C_7 = & K_7 K_8 K_9 + K_6 (K_9 + K_8 + K_7) K_5 + (K_9 + K_8 + K_7 + K_6 + K_2 + K_0) \mathbf{P}_3 \\
& + (K_7 K_9 + K_7 K_8 + K_9 K_8) (K_0 + K_1 + K_2 + K_3 + K_4 + K_5 + K_6) \\
& + ((K_6 + K_5) (K_9 + K_8 + K_7) + K_5 K_6) (K_0 + K_1 + K_2 + K_3 + K_4) \\
& + K_3 (K_0 + K_2) (K_9 + K_8 + K_7 + K_6 + K_5 + K_4) + \frac{\mu}{S^*} K_2 K_9 + \mathbf{P}_2 \\
& + ((K_1 + K_4) (K_0 + K_2) + K_3 K_4) (K_9 + K_8 + K_7 + K_6 + K_5) \\
& + (K_8 + K_7 + K_6 + K_5 + K_4 + K_3 + K_1) \mathbf{P}_1,
\end{aligned}$$

$$\begin{aligned}
C_8 = & (K_9 + K_8 + K_7 + K_6) (K_0 + K_1 + K_2 + K_3 + K_4 + K_5) + K_1 (K_2 + K_0) \\
& + K_5 (K_0 + K_1 + K_2 + K_3 + K_4) + K_9 (K_6 + K_7 + K_8) + K_8 (K_6 + K_7) \\
& + K_4 (K_0 + K_2 + K_3) + K_3 (K_0 + K_2) + K_6 K_7 + \mathbf{P}_1 + \mathbf{P}_3,
\end{aligned}$$

and

$$C_9 = K_0 + K_1 + K_2 + K_3 + K_4 + K_5 + K_6 + K_7 + K_8 + K_9.$$

Consequently, if $R_v \leq 1$ and inequalities (11)–(13) are true, we have $C_{i \in \{0,1,\dots,9\}} > 0$.

Using a technique similar to the one previously employed, the coefficients of the characteristic polynomial for the Jacobian matrix at the endemic equilibrium $J(E_1)$ can be shown to be positive if $R_v > 1$.

References

- [1] Alimerina, H., Abloui, N.L., Maamar, M.H., Bouzid, L., Tabharit, L. and Belhamiti, O. *Mathematical modeling of the impact of vaccination on infected linked Covid-19 disease*, International Conference on Recent Advances in Mathematics and Informatics (ICRAMI). IEEE, 2021.
- [2] Almatroud, A.O., Djenina, N., Ouannas, A., Grassi, G. and Al-Sawalha, M.M. *A novel discrete-time COVID-19 epidemic model including the compartment of vaccinated individuals*, Math. Biosci. Eng. 19 (2022), 12387–12404.
- [3] Balabdaoui, F. and Mohr, D. *Age-stratified discrete compartment model of the COVID-19 epidemic with application to Switzerland*, Sci. Rep. 10(1) (2020), 1–12.
- [4] Cavanaugh, A.M., Spicer, K.B., Thoroughman, D., Glick, C. and Winter, K. *Reduced risk of reinfection with SARS-CoV-2 after COVID-19 vaccination—Kentucky, May–June 2021*, Morb. Mortal. Wkly. Rep. 70(32) (2021), 1081.
- [5] Chitnis, N., Hyman, J.M. and Cushing, J.M. *Determining important parameters in the spread of malaria through the sensitivity analysis of a mathematical model*, Bull. Math. Biol. 70 (2008), 1272–1296. <https://doi.org/10.1007/s11538-008-9299-0>
- [6] Cui, J., Li, F. and Shi, Z.L. *Origin and evolution of pathogenic coronaviruses*, Nat. Rev. Microbiol. 17(3) (2019), 181–192.

- [7] Dammann, O., Gray, P. and Gressens, P., Wolkenhauer, O. and Leviton, A. *Systems epidemiology: What's in a name?*, Online J. Public Health Inform. 6(3) (2014).
- [8] De la Sen, M., Alonso-Quesada, S. and Ibeas, A. *On a discrete SEIR epidemic model with exposed infectivity, feedback vaccination and partial delayed re-susceptibility*, Mathematics, 9(5) (2021), 520.
- [9] De la Sen, M., Alonso-Quesada, S., Ibeas, A. and Nistal, R. *On a discrete SEIR epidemic model with two-doses delayed feedback vaccination control on the susceptible*, Vaccines, 9 (2021), 398.
- [10] Diekmann, O., Heesterbeek, J.A.P. and Metz, J.A. *On the definition and the computation of the basic reproduction ratio R_0 in models for infectious diseases in heterogeneous populations*, J. Math. Biol. 28 (1990), 365–382.
- [11] Imperial College COVID-19 Response Team, *Impact of non-pharmaceutical interventions (NPIs) to reduce COVID-19 mortality and healthcare demand*, 20 (10.25561) (2020), 77482.
- [12] Ivorra, B., Ferrández, M.R., Vela-Pérez, M. and Ramos, A.M. *Mathematical modeling of the spread of the coronavirus disease 2019 (COVID-19) taking into account the undetected infections. The case of China*, Commun. Nonlinear Sci. Numer. Simul. 88 (2020), 105303.
- [13] Killerby, M.E., Biggs, H.M., Midgley, C.M., Gerber, S.I. and Watson, J.T. *Middle East respiratory syndrome coronavirus transmission*, Emerg. Infect. Dis. 26(2) (2020), 191.
- [14] Kranz, J. and Hau, B. *Systems analysis in epidemiology*, Annu. Rev. Phytopathol. 18(1) (1980), 67–83.
- [15] Krishna, M.V. *Mathematical modelling on diffusion and control of COVID-19*, Infect. Dis. Model., 5 (2020), 588–597.
- [16] Ksiazek, T.G., Erdman, D., Goldsmith, C.S., Zaki, S.R., Peret, T., Emery, S., Tong, S., Urbani, C., Comer, J.A., Lim, W. and Rollin, P.E.

- A novel coronavirus associated with severe acute respiratory syndrome*, N. Engl. J. Med., 348(20) (2003), 1953–1966.
- [17] Liu, Y., Yan, L.M., Wan, L., Xiang, T.X., Le, A., Liu, J.M. and Zhang, W. *Viral dynamics in mild and severe cases of COVID-19*, Lancet Infect. Dis. 20(6) (2020), 656–657.
- [18] Morgan, G., de Azambuja, E., Punie, K., Ades, F., Heinrich, K., Personeni, N., Rahme, R., Ferrara, R., Pels, K., Garassino, M. and von Bergwelt-Baildon, M. *OncoAlert round table discussions: The global COVID-19 experience*, JCO Global Oncology, 7 (2021), 455–463.
- [19] Peiris, J.S., Guan, Y. and Yuen, K. *Severe acute respiratory syndrome*, Nat. Med. 10(12) (2004), S88–S97.
- [20] Rabitz, H., Kramer, M. and Dacol, D. *Sensitivity analysis in chemical kinetics*, Annu. Rev. Phys. Chem. 34 (1983), 419–461.
- [21] Ramosa, A.M., Ferrández, M.R., Vela-Pérez, M. and Ivorra, B. *A simple but complex enough θ -SIR type model to be used with COVID-19 real data. Application to the case of Italy*, Phys. D: Nonlinear Phenom. 421 (2021), 132839.
- [22] Van den Driessche, P. and Watmough, J. *Reproduction numbers and sub-threshold endemic equilibria for compartmental models of disease transmission*, Math. Biosci. 180 (2002), 29–48. [https://doi.org/10.1016/S0025-5564\(02\)00108-6](https://doi.org/10.1016/S0025-5564(02)00108-6).
- [23] World Health Organization, *Naming the coronavirus disease (COVID-19) and the virus that causes it*, Braz. J. Implantol. Health Sci. 2(3) (2020).
- [24] World Health Organization, *Novel Coronavirus (2019-nCoV): situation report 1*, <https://www.who.int/docs/default-source/coronaviruse/situation-reports/20200121-sitrep-1-2019-ncov.pdf> (accessed on 20 January 2023).
- [25] World Health Organization, *Novel Coronavirus (2019-nCoV):situation report 51*, <https://www.who.int/docs/default-source/>

- [coronaviruse/situation-reports/20200311-sitrep-51-covid-19.pdf](#) (accessed on 20 January 2023).
- [26] World Health Organization, *Novel Coronavirus (2019-nCoV):situation report 75*, <https://www.who.int/docs/default-source/coronaviruse/situation-reports/20200404-sitrep-75-covid-19.pdf> (accessed on 20 January 2023).
- [27] World Health Organization, *Weekly epidemiological update on COVID-19 - 21 December 2021*, <https://www.who.int/publications/m/item/weekly-epidemiological-update-on-covid-19---21-december-2021> (accessed on 20 January 2023).
- [28] World Health Organization, *Weekly epidemiological update on COVID-19 09 November 2022*, <https://www.who.int/publications/m/item/weekly-epidemiological-update-on-covid-19---9-november-2022> (accessed on 20 January 2023)
- [29] Xu, M., Wang, D., Wang, H., Zhang, X., Liang, T., Dai, J., Li, M., Zhang, J., Zhang, K., Xu, D. and Yu, X. *COVID-19 diagnostic testing: technology perspective*, Clin. Transl. Med. 10(4) (2020), e158.
- [30] Yang, B., Yu, Z. and Cai, Y. *The impact of vaccination on the spread of COVID-19: Studying by a mathematical model*, Phys. A: Stat. Mech. 590 (2022), 126717.
- [31] Yavuz, M.Ö., Coşar, F., Günay, F. and Özdemir, F.N. *A new mathematical modeling of the COVID-19 pandemic including the vaccination campaign*, Open Journal of Modelling and Simulation, 9(3) (2021), 299–321.
- [32] Zaki, A.M., Van Boheemen, S. , Bestebroer, T.M., Osterhaus, A.D. and Fouchier, R.A. *Isolation of a novel coronavirus from a man with pneumonia in Saudi Arabia*, New Engl. J. Med. 367(19) (2012), 1814–1820.